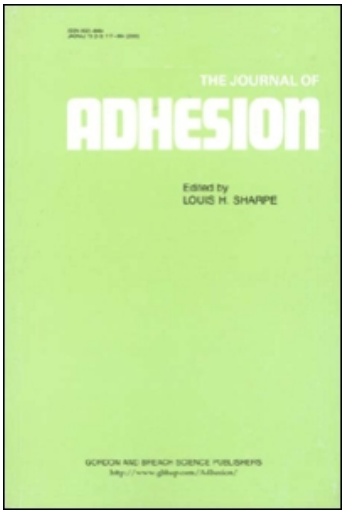

The Journal of Adhesion

Publication details, including instructions for authors and subscription information:
http://www.informaworld.com/smpp/title~content=t713453635

Influence of the Spew Fillet and other Parameters on the Stress Distribution in the Single Lap Joint

A. D. Crocombe[a]; R. D. Adams[a]
[a] Department of Mechanical Engineering, University of Bristol, Bristol, England

To cite this Article Crocombe, A. D. and Adams, R. D.(1981) 'Influence of the Spew Fillet and other Parameters on the Stress Distribution in the Single Lap Joint', The Journal of Adhesion, 13: 2, 141 — 155
To link to this Article: DOI: 10.1080/00218468108073182
URL: http://dx.doi.org/10.1080/00218468108073182

J. Adhesion, 1981, Vol. 13, pp. 141–155
0021–8464/81/1302–0141 $06.50/0

Printed in Great Britain

Influence of the Spew Fillet and other Parameters on the Stress Distribution in the Single Lap Joint

A. D. CROCOMBE and R. D. ADAMS†

Department of Mechanical Engineering, University of Bristol, Bristol BS8 1TR, England

(*Received June 16, 1981*)

Even the most recent closed form analyses of single lap joints assume that the adhesive terminates in a square end. In practice a fillet of adhesive (hereafter called the spew) usually forms at the overlap ends. This spew can considerably reduce peak adhesive stresses and so strengthen the joint. An investigation has been made into the role of the spew for a wide range of joint parameters.

The stress distribution across the adhesive thickness was also considered, and was found to be essentially uniform over a large part of the overlap length. However, near the overlap end, the stress variation across the thickness can be high, resulting in higher stresses and so lower strengths than would be expected considering average stress levels in the joint, but even after including the effect of this variation the maximum adhesive stresses have usually been found to be considerably lower than corresponding peak values predicted by closed form analysis of square ended joints.

NOTATION

$[B]$	Strain displacement array
$2C$	Overlap length
$[D]$	Elastic modulus array
E	Tensile modulus
K	Bending moment factor
$[K]$	Stiffness array
L	Adherend length
M	Bending moment
P	Applied load/unit width
$\bar{R}$	Force array
T	Thickness
v	Volume
α	Constant
$\bar{\delta}$	Displacement array

† To whom any communication should be sent.

$\bar{\varepsilon}$ Strain array
ν Poisson's ratio
σ_y Adhesive peel stress
σ_{prin} Adhesive principal stress
σ_{max} *Maximum* adhesive principal, peel or shear stress
σ_{av} *Average maximum* value of adhesive stress
$\bar{\sigma}$ Stress array
τ_{xy} Adhesive shear stress

Subscripts *a* and *b* refer to adherend and adhesive respectively. Superscript * refers to a virtual amount of that quantity.

INTRODUCTION

The relative ease of manufacture and its use in structural applications has made the single lap joint one of the most frequently used adhesive tests. Generally, it is not possible to predict the joint strength unless the adhesive stress state is known. Figure 1 outlines the notation used to define the geometric parameters of the single lap joint and defines the adhesive stress system. In this work, three adhesive stresses are considered, peel (σ_y) and shear (τ_{xy}) stress (shown in Figure 1), and the principal stress.

Adhesive stresses in single lap joints are caused by three main factors:

a) differential straining of the adherends causing a shear stress distribution in the adhesive which is a maximum at the ends of the overlap;

b) offset loading of the lap joint which causes the loaded adherend to bend

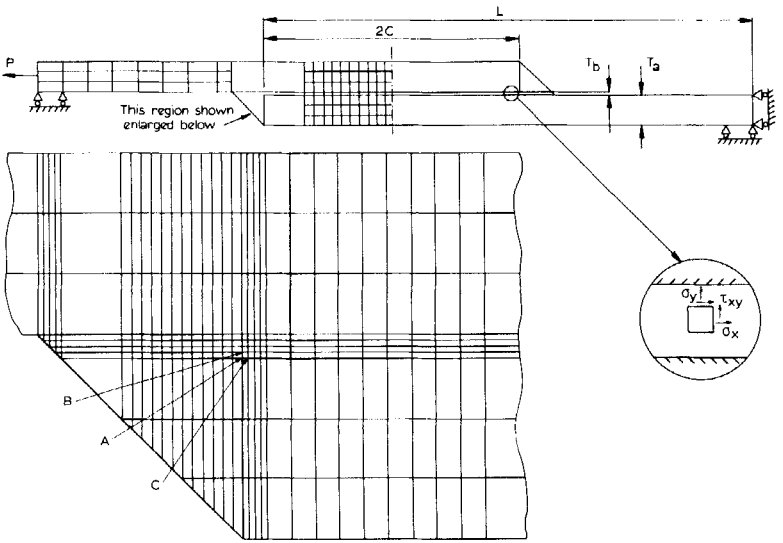

FIGURE 1 Single lap joint geometry and finite element mesh.

adjacent to the overlap region; this causes peel stresses in the adhesive which are a maximum at the overlap ends where the effect of the bending is to separate the adherends;

c) end effects such as the adhesive free surface, spew, and material and geometric discontinuities which all affect the stresses at the overlap ends.

Volkersen[1] was among the first to model differential straining of the adherends while Goland and Reissner[2] included the effect of adherend bending. This was done by considering the overlap region of the lap joint separately, calculating the loads and moments exerted by the free adherend, and using these as boundary conditions. These boundary conditions are still used in most recent analyses of lap joints. Both of these early approaches are limited because the peel and shear stresses are assumed constant across the adhesive thickness, the shear stress is a maximum (and not zero) at the overlap end (a free surface), and the shear deformation of the adherends are neglected.

More recently, however, Renton and Vinson[3] and Allman[4] are among authors who have modelled adherends with bending, shear and normal stresses. They have also set the adhesive shear stress to zero at the overlap ends. In addition, Allman assumes a linear variation of peel stress across the adhesive thickness and his analysis has been used here to compare with the finite element results. None of these analyses, however, model the adhesive spew fillet which, as will be shown later, has an important effect on the stress distribution.

An alternative approach is the finite element method. Wooley and Carver[5] were among the first to apply this method to the single lap joint. They carried out a parametric study, investigating the effect of adhesive modulus, overlap length and thickness but still modelled the adhesive as having a square end. Furthermore, no attempt was made to refine the mesh in the regions at the overlap ends. Nonetheless, good correlation was found with closed form analyses. Wang *et al.*[6] also carried out a parametric investigation, using a greater degree of mesh refinement than Wooley and Carver, and showed that the stresses can vary considerably across the adhesive thickness. They also included a type of spew fillet but this was not very realistic as it was restricted to the height of the adhesive layer. Adams and Peppiatt[7] showed that the spew fillet plays an important role in reducing the peak adhesive stresses, both by load transfer before the overlap region and by removing the stress concentration at the adhesive-adherend corner.

Thus, it was the purpose of this work to investigate how a realistic spew fillet affected the adhesive stress distribution over a range of material and geometric properties and, further, to investigate the stress distribution across the adhesive thickness, a parameter which has been assumed to be constant in so many analyses.

METHOD AND OUTLINE OF ANALYSIS

The single lap joint has been analysed using an elastic, plane-strain, two-dimensional, finite element program, which uses rectangular, quadratic, isoparametric elements. Details of the finite element method can be found elsewhere,[8] but the following outlines some of the principles involved. The structure is sub-divided into a number of finite elements, the displacements at discrete points on the element boundaries, called nodes, are the problem variables. By defining the displacement within the element in terms of the nodal displacements ($\bar{\delta}$) it is possible to obtain expressions for strain ($\bar{\varepsilon}$) and stress ($\bar{\sigma}$)

$$\bar{\varepsilon} = [B]\bar{\delta} \tag{1}$$

$$\bar{\sigma} = [D]\bar{\varepsilon} = [D][B]\bar{\delta} \tag{2}$$

By imposing a small virtual displacement ($\bar{\delta}^*$) from the equilibrium position on the structure it is possible to equate the work done by any external forces ($\bar{R}$) with that done by the stresses and strains

$$\bar{\delta}^{*T}\bar{R} = \int_{\text{vol}} \bar{\varepsilon}^{*T}\,\bar{\sigma}\,dv \tag{3}$$

Substituting from Eqs (1) and (2) into Eq. (3) gives

$$\bar{\delta}^{*T}\bar{R} = \bar{\delta}^{*T}\left(\int_{\text{vol}} [B]^T[D][B]\,dv\right)\bar{\delta} \tag{4}$$

Simplifying and re-arranging Eq. (4) yields an expression for the displacements ($\bar{\delta}$) in terms of the forces ($\bar{R}$), the strain-displacement array ($[B]$) and the elastic modulus array ($[D]$)

$$\bar{\delta} = [K]^{-1}\,\bar{R}$$

where

$$[K] = \int_{\text{vol}} [B]^T[D][B]\,dv$$

The integral over the whole region is obtained by a summation of the elemental values, determined using numerical integration. The process can be shown to be equivalent to minimising the total energy of the system.

The accuracy of the solution from a finite element analysis depends upon sufficient mesh refinement; this was achieved by successive refinement of the mesh until a stable stress distribution was obtained. The mesh used in this work and the boundary conditions applied are shown in Figure 1. A 45° spew fillet has been used which extends to the full height of the adhesive and adherend thickness.

The eccentric loading in a single lap joint which causes bending in the loaded adherend makes analysis of the joint non-linear with load since, as the load increases, the adherends bend further; this consequently reduces the bending moment per unit load acting on the overlap region, see Figures 2(a) and (b). Goland and Reissner[2] accounted for this by introducing a bending moment factor, K, linking the moment at the overlap, M, to the applied load, P, such that

$$M = KP\frac{T_a}{2}$$

where $K = (1+2\sqrt{2}\tanh(\alpha C))^{-1}$ (5)

$$\alpha = \frac{1}{T_a}\left[\frac{3(1-\nu_a^2)P}{2E_aT_a}\right]^{1/2}$$

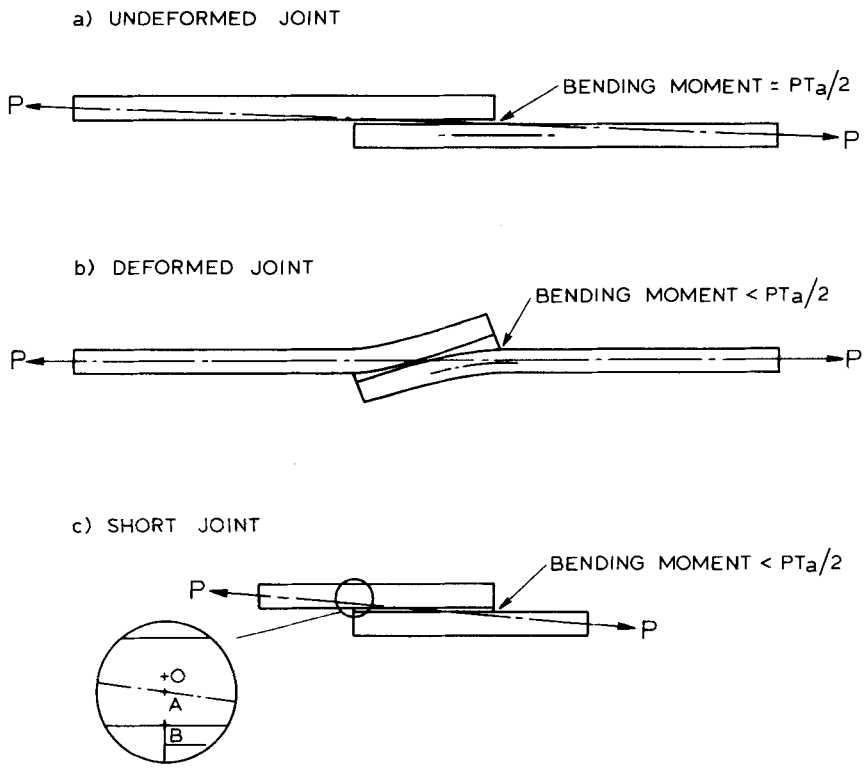

FIGURE 2 Illustrating a way of representing Goland and Reissner's bending moment factor geometrically.

In a finite element analysis of a single lap joint, it is possible to include this effect by shortening the adherends as shown in Figure 2(c), after Peppiatt[9]

$$K = \frac{OA}{OB} = \frac{(L-2C)(T_a+T_b)}{T_a(L-C)} \tag{6}$$

Thus, for all the configurations analysed, the bending moment factor can be calculated from Eq. (5) and the effective adherend length determined using Eq. (6).

The parameters investigated include the ratio of adherend to adhesive modulus (hereafter referred to as the "modulus ratio"), the adhesive thickness, the adherend thickness, the overlap length and the load magnitude. Further details are summarised in Table I. Values of all the parameters are set to the standard values unless otherwise specified. These standard values represent typical aluminium-epoxy single lap joints. To facilitate the generation of the finite element meshes, a program was written which produced varying degrees of mesh refinement in a single lap joint of any geometric or material configuration.

TABLE I

Details of Parameters Investigated

Adhesive modulus GPa	Adherend modulus GPa	Overlap length mm	Load per unit width N mm^{-1}	Adhesive thickness mm	Adherend thickness mm
14.00	70.00†	7.50	0.75	0.06	5.00
7.00		12.50†	37.50†	0.12	2.50
4.67		25.00	56.25	0.20†	1.50†
2.80†				0.30	1.00
1.40				0.60	0.50
0.70					
0.35					
0.14					

† These are standard values in this work.

RESULTS

Comparison with closed form analyses

Analyses of the standard configuration (defined in Table I) with and without a spew fillet were made. Low loads were applied (0.075 N mm^{-1}) as this should provide the best correlation with closed form analyses, since the bending moment factor, from Eq. (5), is nearly unity.

Figure 3 shows how the stresses vary across the adhesive thickness for the joint with a spew fillet. These stresses remain essentially uniform to within a

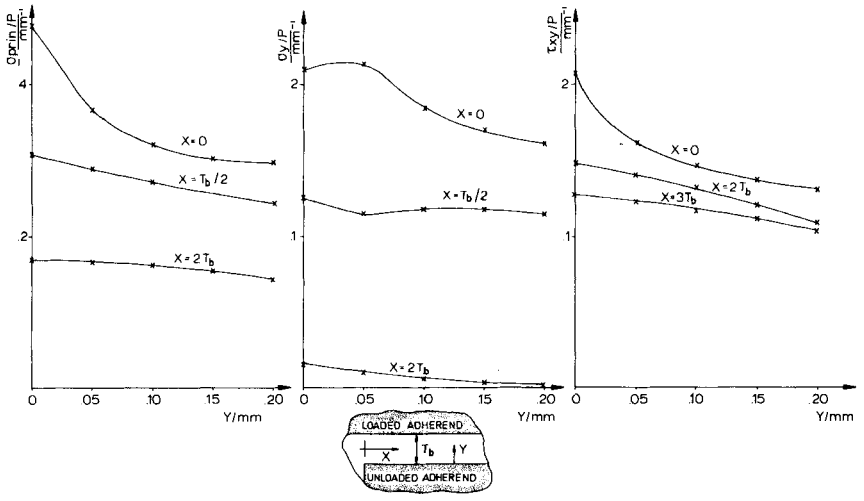

FIGURE 3 Variation of adhesive principal (σ_{prin}), peel (σ_y) and shear (τ_{xy}) stresses across the adhesive thickness (y) at various distances (x) from the overlap ends.

few adhesive thicknesses from the overlap end. The principal and peel stresses are seen to smooth out more rapidly than the shear stresses. A possible explanation for this stress variation across the adhesive thickness near the overlap end is the discontinuity caused by the unloaded adherend.

Figure 4 shows the same stresses plotted against distance from the overlap end along three planes in the adhesive parallel to its length, on the unloaded adherend-adhesive interface, on the adhesive central plane and on the loaded adherend-adhesive interface. Again the variation in the stresses increases towards the overlap end. The maximum value of the shear stress is seen to occur just within the overlap and this is discussed later. The peak in the stress distributions appears to shift from the overlap end further into the spew as the distance of the plane of the stresses from the unloaded adherend increases. This is probably because load transfer in the lap joint does not occur perpendicularly across the adhesive thickness, the maximum loads are likely to travel from the loaded adherend before the overlap and across the adhesive to the corner of the unloaded adherend, the positions of the peak stresses may correspond with this load line.

The positions of the maximum of all the adhesive stresses occur under the overlap, the maximum principal stress being at the unloaded adherend corner, acting at about 45° to the longitudinal axis of the joint (a feature first noted by Adams and Peppiatt[7]), the maximum peel stress being at the overlap end just within the adhesive layer, and the maximum shear stress being on the adhesive-adherend interface at a small distance from the overlap end: these

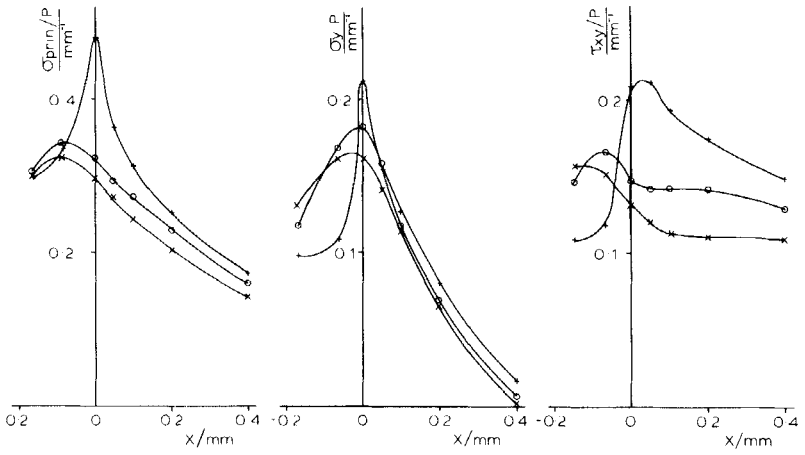

FIGURE 4 Variation of adhesive principal (σ_{prin}), peel (σ_y) and shear (τ_{xy}) stresses with distance from the overlap end (x) at various longitudinal planes through the adhesive (+ unloaded adherend interface; o adhesive mid-plane; x loaded adherend interface).

points are labelled A, B and C respectively in Figure 1, and do not vary widely over the range of configurations analysed.

Analysis of a square-ended joint indicates low values of peel stress in the adhesive adjacent to the unloaded adherend corner; this is discussed later, but it may explain the flattening in the distribution of the peel stress at the overlap end ($x = 0$) in Figure 3(b).

The maximum adhesive shear stress may occur just within the overlap because adhesive shear stresses in the spew are low, thus reducing the values of the shear stress at the overlap end. Comparison was made with the analysis of Allman[4] by averaging the finite element stresses across the adhesive thickness. Results for adhesive, peel and shear stresses are shown in Figure 5. The

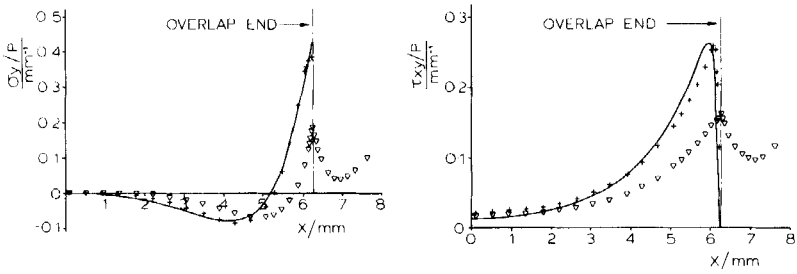

FIGURE 5 Variation of averaged adhesive peel (σ_y) and shear (τ_{xy}) stresses with distance (x) from the centre of the overlap (– Allman[4]; + finite element with square end; V finite element with spew fillet).

beneficial effect of the spew fillet can be seen since the peak peel and shear stresses are reduced to 44% and 61% of the closed form values respectively. The finite element stresses from the square-ended joint compare well with those predicted by Allman;[4] the peel stress at the overlap end probably differs from Allman's because he assumed a linear variation of peel stress across the adhesive thickness, while at the overlap ends the distribution has been found to be more exponential than linear in form, and so the linear approximation results in higher averaged stresses than are actually present. For the finite element analysis with a spew fillet, the stresses again increase as they reach the end of the spew, the sharp adhesive-adherend corner acting as a stress concentration. In practice, the spew fillet will blend smoothly, so eliminating this point of stress concentration, which therefore creases to be of practical interest. The remainder of this paper considers the effect of varying the different parameters, outlined in Table I, on the adhesive stresses, averaged across the bond thickness (assessing the role of the spew fillet by comparing values with those for a square-ended joint[4]) and on the variation of the stress across the adhesive thickness. The variation of the stress across the adhesive thickness has been defined as:

$$(\sigma_{max} - \sigma_{av})/\sigma_{av}$$

where σ_{max} is the maximum value of that stress.
σ_{av} is the average value of that stress.

It is always determined at the section where that stress is a maximum, and so enables the maximum value of any adhesive stress to be obtained from the average value.

The stresses used are nodal stresses (on element corners) obtained by extrapolation from the values at the gauss points (points of numerical integration) within the element. The method used is a standard technique introduced by Hinton *et al.*[10] In the ensuing sections the *maximum* stress refers to the highest value of the finite element adhesive stress while the *averaged maximum* stress refers to the average of the finite element stresses across the thickness at the point of the maximum stress. This *averaged maximum* stress is often the peak value of the averaged stress distribution, however, even when this is not the case it is a good measure of the averaged stress level and the trends obtained in Figure 6 would be repeated if peak values of averaged stress were used.

Variation of modulus ratio

In this series of tests the modulus ratio was varied between 5 and 500 (Table I) this being considered to be a representative range of values (25 being a typical

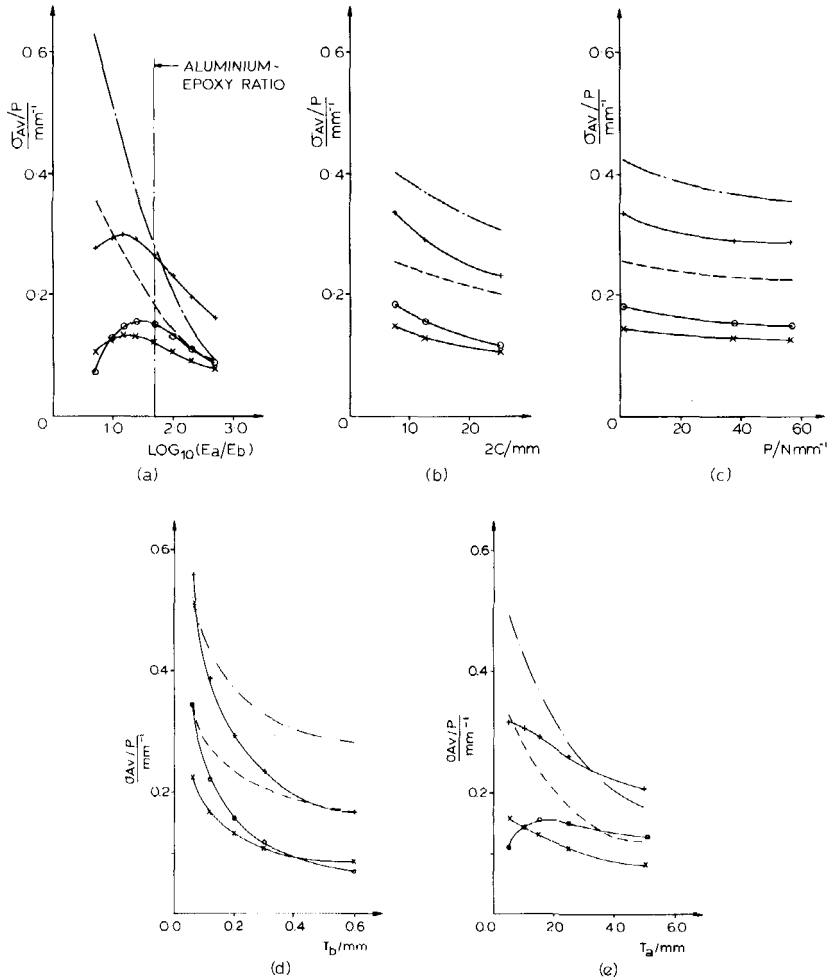

FIGURE 6 Variation of the adhesive *averaged maximum* stresses (σ_{av}) with (a) modulus ratio (E_a/E_b); (b) overlap length ($2C$); (c) applied load (P); (d) adhesive thickness (T_b); (e) adherend thickness (T_a). (– · – peel[4]; – – – shear[4]; + principal; ○ peel; × shear stresses).

value for aluminium-epoxy joints). The Goland and Reissner bending moment factor is calculated (it is constant for this series of tests) and the adherend length set to the appropriate value. Closed form analyses predict a steady increase in the averaged adhesive stress level with decreasing modulus ratio (increasing adhesive stiffness). This occurs because as the adhesive becomes stiffer, more load passes through the region at the overlap ends, thus raising the stress level.

Finite element results for a lap joint with a spew fillet, see Figure 6(a), indicate that the *averaged maximum* adhesive stresses increase with decreasing modulus ratio up to a limiting value, after which they decrease again. This is due to the spew fillet, since as the adhesive modulus increases so proportionately more load can be transferred through the spew, thus reducing the load and hence the stresses in the overlap region. Closed form analyses of square-ended lap joints predict that the peak adhesive stresses approach an asymptotic value with increasing adhesive stiffness. Thus it is suggested that above a certain adhesive modulus the stress reduction caused by load transfer in the spew is greater than the stress increase caused by the stiffer adhesive layer and hence the peak stresses are reduced. Comparison between the *averaged maximum* finite element peel and shear stresses with those predicted by Allman[4] (Figure 6(a)) indicates the effect of the spew fillet on the stress distribution. The differences between the two analyses are greatest at low modulus ratios because of the greater load-carrying capacity of the spew. The *averaged maximum* finite element stresses range from 12% to 93% and from 30% to 82% of the closed form values for peel and shear stresses respectively.

Figure 7(a) gives details of the stress variations across the adhesive thickness. The variations in all the stresses are seen to decrease with increasing modulus ratio, breaks in the curves occur because the position of the *maximum* stress changes from A to B and from C to A (see Figure 1) for the peel and shear stresses respectively. In fact these changes are not abrupt, the sudden change arises because the stresses can only be considered at discrete points, *i.e.* in relation to the finite element mesh. This decrease in variation is possibly caused by the reduced load carrying capacity of the spew which would tend to reduce the adhesive stresses in the spew adjacent to the unloaded adherend and hence reduce the variation in adhesive stress between the loaded and

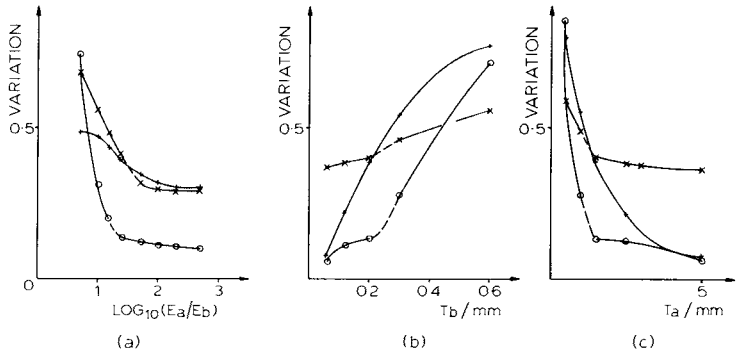

FIGURE 7 Showing how the stress variation changes with (a) modulus ratio (E_a/E_b); (b) adhesive thickness (T_b); (c) adherend thickness (T_a). (+ principal, ○ peel, × shear stresses).

unloaded adherends. The variation can be seen, Figure 7(a), to reduce from 48% to 30% from 74% to 10% and from 68% to 29% for principal, peel and shear stresses respectively.

Variation of overlap length and loading

The range of overlap lengths and loads applied are summarised in Table I. The adherend length was calculated by determining the appropriate Goland and Reissner bending moment factor. Closed form analyses of a square-ended joint indicate that the peak adhesive stress per unit load decreases with increasing overlap length and applied load. Increasing the overlap length reduces the adherend strains and so the adhesive stresses while increasing the load causes greater adherend bending, which reduces the bending moment (for a unit load) on the overlap region and hence reduces the adhesive stresses.

Figures 6(b) and (c) show the variation of the *averaged maximum* adhesive stresses with overlap length and loading, the trend predicted by closed form analyses of square-ended joints, discussed above, applies here also. Comparison with the peak stresses predicted by Allman[4] shows that for increasing overlap length the values of the *averaged maximum* finite element peel and shear stresses range from 46% to 38% and from 58% to 53% of the closed form values respectively. A similar comparison shows that the reduction from the closed form value is essentially independent of the applied load, values of *averaged maximum* finite element stresses being about 43% and 57% of the closed form peel and shear stress values respectively. This indicates that the effect of the spew fillet is unchanged as the load increases but that it plays a greater role as the overlap length increases. Possibly as the overlap increases the joints become more flexible and so the spew fillet which is unchanged has an increasingly dominant effect.

Neither the variation of adhesive stresses across the thickness nor the position of *maximum* stress change significantly with overlap length or load. The variation of stress across the thickness is about 39% for the principal stress, 13% for the peel stress and 40% for the shear stress.

Variation of adhesive thickness

Table I shows that the adhesive thickness was varied from 0.06 mm to 0.6 mm, this being typical of most structural glue line thicknesses. Closed form analyses of square-ended joints predict decreasing stress levels with increasing adhesive thickness because, as the layer becomes thicker, its flexibility with respect to the rest of the system increases and hence less load is transferred at the overlap ends, resulting in lower stresses in the adhesive. Figure 6(d) shows how the *averaged maximum* adhesive stresses vary with adhesive thickness, the trend of decreasing stress levels with increasing adhesive thickness discussed above can

be seen. The effect of the spew fillet can be seen by comparing peak stresses from Allman[4] with the finite element values (Figure 6(d)). The *averaged maximum* finite element stresses range between 65% and 25% of the closed form value for peel stresses and between 67% and 51% of the closed form value for shear stresses, the difference between the two analyses, *i.e.* the effect of the spew, being greater at higher adhesive thicknesses. A possible explanation for this increasing discrepancy is that as the size of the spew fillet increases with glue line thickness so it carried proportionately more load, thus reducing the load transferred, and hence the stresses, in the overlap region.

Figure 7(b) shows the variation of the stresses across the adhesive thickness, at the point of the maximum adhesive stress, for varying adhesive thicknesses. The stress variation increases with increasing thickness, from 7% to 77% for the principal stress, from 6% to 71% for the peel stress and from 37% to 55% for the shear stress. Breaks in the peel and shear stress curves occur because the position of *maximum stress* changes, as the thickness is increased, from B to A and from C to A (Figure 1) respectively. A possible explanation for this increase in stress variation is that when the adhesive layer is thin it approximates to the case of plane (uniform) stress and only as the adhesive becomes thicker can the stress vary significantly across the thickness. This trend is supported by Allman's results which predict an increase in the variation of the stress with increasing adhesive thickness.

Variation of adherend thickness

Values of adherend thickness ranging from 5.0 to 0.5 mm were considered (Table I). Closed form analyses predict an increase in adhesive stress levels with decreasing adherend thickness. This is largely because, as the adherend thickness decreases, to support the same load, the adherend stresses, and so strains, increase; this then causes higher adhesive stresses.

Figure 6(e) shows that the *averaged maximum* finite element stresses essentially follow the same pattern as the square-ended joint stresses, except that at low adherend thicknesses the *averaged maximum* peel stresses tend to decrease. Further, comparison between peak stresses from Allman[4] and the finite element values (Figure 6(e)) show that the effect of the spew fillet is more pronounced at low adherend thickness, a possible explanation for the decrease in peel stresses at low thicknesses. The *averaged maximum* finite element stresses range from 73% to 22% and from 69% to 48% of the closed form values for peel and shear stresses respectively as the adherend thickness decreases. A possible explanation is that although the size of the spew fillet reduces with decreasing adherend thickness, the adherend itself becomes more flexible and a higher proportion of the load is transferred through the spew, increasing the difference between finite element and closed form results.

Figure 7(c) shows the variation of stress across the adhesive thickness increases with decreasing adherend thickness, from 7% to 79% for principal stresses, from 6% to 85% for peel stresses and from 36% to 60% for shear stresses. Again the break in the peel and shear stress curves is because the position of *maximum* adhesive stress (at which the variation is calculated) changes from B to A and from C to A (Figure 1) respectively as the adherend thickness decreases. This trend, also evidenced in Allman's closed form analysis, is possibly caused by the inability of the adherend to constrain the adhesive to a uniform stress as the thickness reduces, a similar effect to increasing the adhesive thickness (see last section). This increased variation at low adherend thicknesses means that although the *averaged maximum* peel stress increases and then decreases with decreasing adherend thickness actual values of *maximum* adhesive stress increase continuously, unlike the tests involving modulus ratio changes, where the *maximum* stresses followed the same pattern as the *averaged maximum* stresses.

CONCLUSIONS

A study of the effect of the interaction between a realistic spew fillet and other joint parameters on the adhesive stress distribution in a single lap joint has been undertaken for a wide range of geometric and material parameters using a linear elastic finite element program. A comparison has been made throughout with a closed form solution[4] (for a square edged joint) by averaging the stress across the adhesive thickness. The spew fillet always reduces the stress levels from those predicted by closed form analysis (which can only accommodate a square-ended joint) and for parameters such as modulus ratio and adherend thickness, even the trend of the stress levels is changed. A reason for the effect of the spew fillet is that it transfers load that would otherwise be transferred in the overlap region and also modifies the stress concentration found in a square-ended joint. Values for *averaged maximum* adhesive peel and shear stresses for typical aluminium-epoxy single lap joints are about 43% and 57% of the closed form values[4] respectively, although these values have been shown to reduce to 12% and 30% for low modulus ratios and to about 24% and 50% for low adherend thickness or high adhesive thickness.

The variation in stress across the adhesive thickness (often assumed constant) has also been considered. It is not affected by changes in overlap length or loading, variations in principal, peel and shear stresses remaining at about 39%, 13% and 40% respectively. This suggests that the variation is mainly induced by the presence of the end of the unloaded adherend. Further, changes in both modulus and thickness ratios affect these variations. The

principal, peel and shear variations ranging from 48% to 30%, 74% to 10% and 68% to 29% as the modulus ratio increases, and from about 7% to 78%, 6% to 78% and 37% to 58% as either the adhesive thickness increases or the adherend thickness decreases. Using the data from Figures 6 and 7, it can be seen that although the variation sometimes causes *maximum* stresses to be considerably higher than the *average maximum* values, the stress reducing effect of the spew fillet almost always maintains the maximum stresses (the stresses likely to determine the joint strength) below the levels predicted by closed form analyses of square-ended joints. These differences are higher for peel than shear stresses. In the finite element analysis of the standard configuration (a typical single lap joint) maximum peel and shear stresses are about 48% and 78% of their respective closed form values. These reductions are greatest at low modulus ratios, high adhesive thicknesses, and low adherend thicknesses.

Finally, the position of *maximum* adhesive stress is always found to be within the overlap region.

References

1. O. Volkersen, *Luftfahrtforschung* **15,** 41 (1938).
2. M. Goland and E. Reissner, *J. Appl. Mech., Trans. Am. Soc. Engs.* **66,** A17 (1944).
3. W. J. Renton and J. R. Winson, *J. Adhesion* 7(3), 175 (1975).
4. D. J. Allman, *Tech. Rep. 76024*, Royal Aircraft Establishment, Farnborough, Hants (1976).
5. G. R. Wooley and D. R. Carver, *J. Aircraft* **8,** 817 (1971).
6. S. S. Wang *et al., Res. Rep. R76-2*, Dept. of Matls. Sci. & Eng., M.I.T. (1976).
7. R. D. Adams and N. A. Peppiatt, *J. Strain Anal.* **9,** 185 (1974).
8. O. C. Zienkiewicz, *The finite element method* (McGraw-Hill, New York, 1977), 3rd ed.
9. N. A. Peppiatt, Ph.D. Thesis (University of Bristol, 1974).
10. E. Hinton, F. C. Scott and R. E. Ricketts, *Int. J. Num. Meth. Eng.* **9,** 235 (1975).